Journal of Materials Chemistry A

Accepted Manuscript

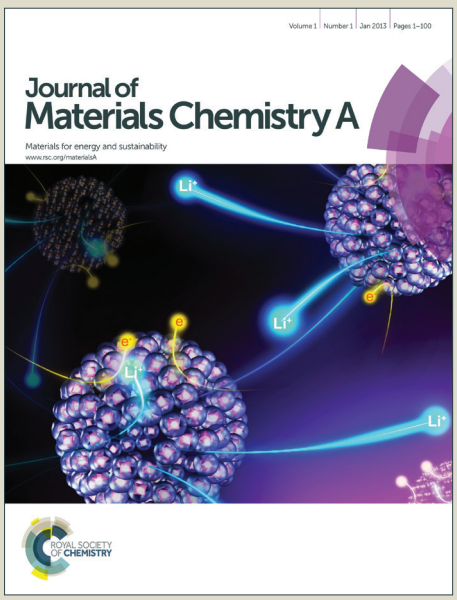

ROYAL SOCIETY OF CHEMISTRY

www.rsc.org/materialsA

Journal Name

RSCPublishing

ARTICLE

Pyrazino[2,3-g]Quinoxaline Dyes for Solar Cell Applications

Cite this: DOI: 10.1039/xoxxoooooox

Li-Peng Zhang,[a,b] Ke-Jian Jiang,*[,a] Gang Li,*[,a] Qian-Qian Zhang,[a,b] and Lian-Ming Yang*[,a]

Received ooth January 2012,
Accepted ooth January 2012

DOI: 10.1039/xoxxoooooox

www.rsc.org/

Pyrazino[2,3-g]quinoxaline was first employed as a π–linker in D-π–A type dyes, exhibiting an unusually broad and intense spectral absorption ranged from the visible to the near infrared region. A power conversion efficiency of 6.86% was achieved in dye-sensitized solar cells.

Introduction

As one of the most promising alternatives to the conventional inorganic photovoltaic devices, dye-sensitized solar cells (DSCs) have attracted intense attention due to their potentially low-cost production and high conversion efficiencies.[1] In the DSC, a monolayer of sensitizer molecules adsorbed on mesoporous oxide film (usually TiO_2) are employed to extend the light absorption window of the photoanode in the solar spectral region, exerting a significant influence on the power conversion and stability of the devices. DSCs with ruthenium complexes achieved a high power conversion efficiency of up to 12%.[2] On the other hand, a large number of organic dyes have been developed over the past two decades because of their molecularly tailoring flexibility, raw-material abundance, and high efficiencies comparable to Ru complexe-based DSCs.[3]

Organic dyes used in DSCs commonly consist of an electron donor and an electron acceptor being linked by a π-conjugation linker (i.e., typically D–π–A configuration). Accordingly, different π-conjugated linkers have been utilized to bridge a donor (such as triarylamines) and an acceptor (like cyanoacrylic acid).[3] In fact, the π-linker is of paramount importance in tuning the energy gap as well as the electronic and steric properties of the dye molecule, which would strongly affect the device performances. Especially, such linkers with the electron-poor property as benzothiadiazole,[4] benzotriazole,[5] quinoxaline,[6] diketopyrrolopyrrole,[7] squaraine,[8] boradiazaindacene,[9] isoindigo,[10] and phthalimide[11] were preferred to develop low-band gap sensitizers for improving light harvesting ability in the red and near-infrared region.

Pyrazino[2,3-g]quinoxaline (PQ**)** is an electron-deficient and rigid unit, and has been extensively employed as a building block in combination with different electron-donating units in constructing low-band gap polymers for bulk heterojunction solar cells.[12] In this article, we first introduced the pyrazino[2,3-g]quinoxaline into two small molecular organic dyes for DSCs, where pyrazino[2,3-g]quinoxaline as a linker to bridge a triarylamine donor and a cyanoacrylic acid acceptor. The two dyes were denoted as **PQ-1** and **PQ-2**, as shown in Figure 1.

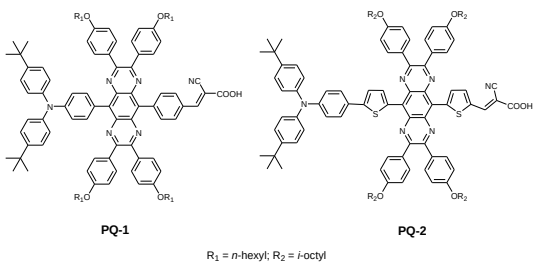

Figure 1. Structures of pyrazino[2,3-g]quinoxaline-bridged donor–acceptor dyes **PQ-1** and **PQ-2**.

The incorporation of PQ in the dye molecules efficiently extends the spectral absorption range in the visible and infrared region due to their electron-deficient and rigid properties. In addition, the rigid and planar PQ favors a charge transfer from triarylamine donor to cyanoacrylic acid acceptor. It should be noted that the dyes with planar and rigid PQ unit may easily aggregate on TiO_2 surface through the cofacial π–π interactions between the macrocycle discs, which would deteriorate the device performances. With this in mind, four lateral bulky alkoxy-substituted phenyl units were specifically introduced onto the planar PQ to reduce the molecular aggregation and increase the solubility. In our experiment, the DSC based on dye **PQ-1** gave the power conversion efficiency of 6.86% under standard AM 1.5 conditions.

Experimental Section

Measurement and characterization

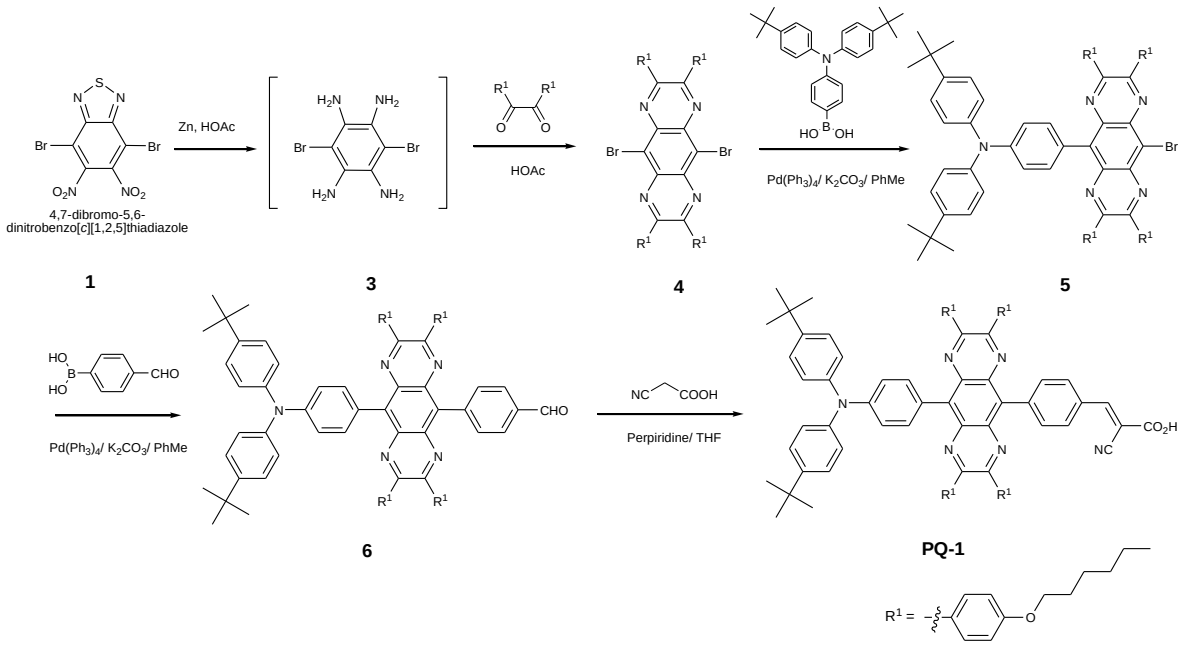

Scheme1 The synthetic route to **PQ-1.**

NMR spectra were recorded on a BRUKER AVANCE 400 MHz instrument. The residual solvent protons (^{1}H) or the solvent carbons (^{13}C) were used as internal standards. ^{1}H NMR data are presented as follows: the chemical shift in ppm (δ) downfield from tetramethylsilane (multiplicity, coupling constant (Hz), integration). The following abbreviations are used in reporting NMR data: s, singlet; d, doublet; t, triplet; q, quartet; and m, multiplet. IR spectra were recorded on a BRUKER EQUINOX55 instrument. UV-vis absorption spectra were recorded on a Shimadzu UV-1800 spectrophotometer. Mass spectra were taken on a Bruker Daltonics Inc. spectrometer. The photocurrent–voltage (I–V) characteristics were recorded at room temperature using a computer-controlled Keithley 2400 source meter under air mass (AM) 1.5 simulated illumination (100 mW cm^{-2}, Oriel, 67005). The action spectra of the monochromatic incident photo-to-current conversion efficiency (IPCE) for solar cells were collected using a commercial setup (PV-25 DYE, JASCO). A 300-W Xenon lamp was employed as the light source for generation of a monochromatic beam. Calibrations were performed with a standard silicon photodiode. IPCE is defined as IPCE (λ) = $hcJ_{sc}/e\varphi\lambda$, where h is Planck's constant, c the speed of light in a vacuum, e the electronic charge, λ the wavelength in meters (m), J_{sc} the short-circuit photocurrent density (A m^{-2}), and φ the incident radiation flux (W m^{-2}).

Materials

All of solvents were purified according to standard methods. All reagents were commercially obtained from Alfa Aesar Chemical Co. and J&K Chemical Co. and used without further purification unless otherwise specified. All manipulations involving air-sensitive reagents were performed in an atmosphere of dry argon. 4,7-Dibromo-5,6-dinitrobenzo[c][1,2,5]thiadiazole (**1**) was synthesized according to the reference procedure.[13]

Synthesis of 4. The compound **1** (0.60 g, 1.6 mmol) was dissolved in glacial acetic acid (30 mL), followed by adding activated zinc powder (2.4 g) in one portion. After stirring at 70 ^{0}C for 1 h, the mixture solution including the intermediate 3,6-dibromo-1,2,4,5-benzenetetramine **3** which was extremely sensitive to air was filtered to remove the unreactive zinc powder. To the filtrate was added 4, 4'-(hexyloxy)benzil (1.3 g, 3.2 mmol) and the mixture was stirred at 100 ^{0}C for another 20 h. After removal of the solvent, the residue was dissolved in dichloromethane (100 mL), washed with saturated $NaHCO_3$ solution (100 mL), water (100 mL), and brine (100 mL), respectively. The organic phase was dried over anhydrous $MgSO_4$, concentrated in vacuum and purified by silica gel column chromatography (eluting with dichloromethane/ petroleum ether, 20/50, v/v) to afford the quinoxaline product **4** (0.33 g, 20%) as an orange solid. M.p.175-177 ^{0}C ^{1}H NMR ($CDCl_3$, 400 MHz): δ 0.92 (t, J = 13.2 Hz, 12H), 1.26–1.54 (m, 24H), 1.78-1.84 (m, 8H), 4.00 (t, J = 12.9 Hz, 8H), 6.91 (d, J = 8.7 Hz, 8H), 7.77 (d, J = 8.7 Hz, 8H). ^{13}C NMR (CDCl3, 100 MHz): δ 160.86, 154.37, 138.17, 131.91, 130.44, 114.41, 68.16, 31.59, 29.17, 25.71, 22.61, 14.05. HR-MS (MALDI): m/z [M]+ cacld for $C_{58}H_{68}Br_2N_4O_4$, 1042.3607; found, 1042.3602.

Synthesis of 5. A mixture of the compound **4** (150 mg, 0.14 mmol), 4-(bis(4-tert-butylphenyl)amino)phenylboronic acid (70 mg, 0.17 mmol), $Pd(PPh_3)_4$ (25 mg, 15 mol% relative to the compound **4**), K_2CO_3 (83 mg, 0.6 mmol) in toluene (20 mL) and H_2O (3 mL) was refluxed for 15 h under a nitrogen

atmosphere. After removal of the solvents, the residue was dissolved in dichloromethane (50 mL), washed with brine (50 mL), and dried over anhydrous $MgSO_4$. After removal of the solvent, the residue was purified by silica gel column chromatography (eluting with dichloromethane/petroleum ether 20/50, v/v) to afford a mixture of compound **5** and the double cross-coupling compound. The mixed products were difficult to separate and thus the crude compound **5** was directly used in the next reaction.

Synthesis of 6. A mixture of the crude compound **5** (150 mg), 4-formylphenylboronic acid (25 mg, 0.17 mmol), $Pd(PPh_3)_4$ (20 mg, 15%mol), K_2CO_3 (69 mg, 0.5 mmol) in toluene (20 mL) and H_2O (3 mL) was refluxed for 15 h under a nitrogen atmosphere. After removal of the solvents, the residue was dissolved in dichloromethane (50 mL), washed with brine (50 mL) and dried over anhydrous $MgSO_4$. After removal of the solvent, the residue was purified by silica gel column chromatography (eluting with dichloromethane/petroleum ether 20/50, v/v) to afford the crude compound **6** (95 mg, 62%) as a brown solid which was unpurified and directly used in the next reaction.

Synthesis of PQ-1. To a solution of the crude compound **6** (95 mg), cyanoacetic acid (10 mg, 0.12 mmol) and tetrahydrofuran (15 mL) was added a few drops of piperdine and then the reaction mixture was refluxed for 8 h under a nitrogen atmosphere. After the completion of the reaction, acetic acid (2 mL) was added into the mixture, and the solvents were removed under a reduced pressure. The residue was dissolved in dichloromethane (50 mL), washed with water (30 mL) and brine (30 mL), respectively. The organic phase was dried over anhydrous $MgSO_4$. After removal of the solvents, the residue was purified by silica gel column chromatography (eluting with methanol–dichloromethane 10/100, v/v) to afford the dye **PQ-1** (56 mg, 56%) as a deep brown solid. M.p.>220 ^{0}C ^{1}H NMR ($CDCl_3$, 400 MHz): δ 0.87–0.93 (m, 12H), 1.25–1.45 (m, 44H), 1.76-1.80 (m, 8 H), 3.94-3.97 (t, J = 11.6 Hz, 8 H), 6.74 (d, J = 7.2 Hz, 4H), 6.81 (d, J = 8.0 Hz, 4H), 7.24–7.34 (m, 10H), 7.57–7.59 (m, 8H), 7.95 (br. s, 2H), 8.17 (br. s, 2H), 8.50 (br. s, 1H). ^{13}C NMR ($CDCl_3$, 100 MHz): δ 160.35, 160.22, 151.41, 150.90, 147.59, 145.73, 145.10, 136.76, 136.31, 135.54, 135.29, 132.24, 132.16, 131.65, 131.50, 131.08, 130.80, 130.39, 129.90, 129.73, 128.65, 128.56, 127.21, 125.98, 124.65, 120.15, 114.36, 114.21, 68.08, 34.36, 33.71, 31.92, 31.62, 31.59, 31.55, 29.78, 29.69, 29.65, 29.60, 29.46, 29.33, 29.26, 29.21, 29.10, 27.22, 25.74, 25.72, 24.77, 22.68, 14.10; IR(KBr) ν 3026, 2969, 2854, 2230, 1716, 1683, 1651, 1558, 1540, 1507 cm^{-1}; HR-MS (MALDI): m/z [M]+ cacld for $C_{94}H_{104}N_6O_6$, 1412.8017; found, 1412.8012.

Table 1 Photophysical properties of **PQ-1** and **PQ-2**

Dye	λ_{max} [a] (nm)	ε (L mol^{-1} cm^{-1})	$E_{0\text{-}0}$ [b] (eV)	$E_{+/0}$ [c] (V)	$E_{+/*}$ [e] (V)	J_{sc} (mA cm^{-2})	V_{oc} (mV)	FF	η [d] (%)
PQ-1	484	31000	1.84	0.93	-0.91	13.13	768	0.68	6.86
	565	8900							
PQ-2	510	24000	1.48	0.95	-0.53	1.86	432	0.43	0.34
	638	11000							

[a] Absorption spectra in CH_2Cl_2 solution (1.0×10^{-5} M) at room temperature; [b] Estimated by using the onset of the UV-vis spectra in dichloromethane; [c] The estimation was determined by subtracting E0-0 from Es+/0. The oxidation potentials of the dyes were measured in CH_2Cl_2 solutions with tetrabutylammoniumhexafluorophosphate ($TBAPF_6$, 0.1 M) as electrolyte, Pt wires as working and counter electrode, Ag/Ag^+ as reference electrode; calibrated with ferrocene/ferrocenium (Fc/Fc^+) as an internal reference and converted to NHE by addition of 630 mV; [e] The estimation was determined by subtracting $E_{0\text{-}0}$ from $E_{s+/0}$; [d] The data were recorded under AM 1.5 G simulated solar light at a light intensity of 100 mW cm^{-2}, and represents the average of three devices.

DSC fabrication

The nanocrystalline TiO_2 pastes (particle size, 20 nm) were prepared using a previously reported procedure.[14] Fluorine doped thin oxide (FTO, 4 mm thickness, 10 ohm sq^{-1}, Nippon Sheet Glass, Japan) conducting electrodes were washed with soap and water, followed by sonication for 10 min in acetone and isopropanol, respectively. Following a drying period, the electrodes were submerged in a 40 mM aqueous solution of $TiCl_4$ for 30 min at 75 ^{0}C, and then washed by water and ethanol. On the electrodes, an 11 μm thick nanocrystalline TiO_2 layer and a 6 μm thick TiO_2 light scattering layer (particle size, 400 nm, PST-400C) were prepared by the screen-printing method. The TiO_2 electrodes were heated at 500 ^{0}C for 30 min, followed by treating with a 40 mM aqueous solution of $TiCl_4$ for 30 min at 75 ^{0}C and subsequent sintering at 500 ^{0}C for 30 min. The thickness of TiO_2 films was measured using a profiler, Sloan, Dektake.

The electrodes were immersed in a dye bath containing 0.2 mM **PQ-1** or **PQ-2** and 20 mM 3α,7α-dihydroxy-5β-cholic acid (chenodeoxycholic acid) in a mixed solvent of 4-*tert*-butanol–acetonitrile–tetrahydrofuran (1:1:0.2, v/v/v) and kept for 24 h at room temperature. The dyed electrodes were then rinsed with the mixed solvent to remove the excess dye. A platinum-coated counter electrode was prepared according to a previous report,[15] and two holes were drilled on its opposite sides. The two electrodes were sealed together with a 25 μm thick thermoplastic Surlyn frame. An electrolyte solution was then introduced through one of the two holes in the counter electrode, and the holes were sealed with the thermoplastic Surlyn. The electrolyte contains 0.68 M dimethyl imidazolium iodide, 0.05 M iodine, 0.10 M LiI, 0.05 M guanidinium thiocyanate, and

0.40 M 4-*tert*-butylpyridine in a mixed solvent of acetonitrile and valeronitrile (85:15, v/v). All the devices were prepared with a photoactive area of about 0.3 cm^2, and a metal mask of 0.165 cm^2 was used to cover the device for photovoltaic property measurements.

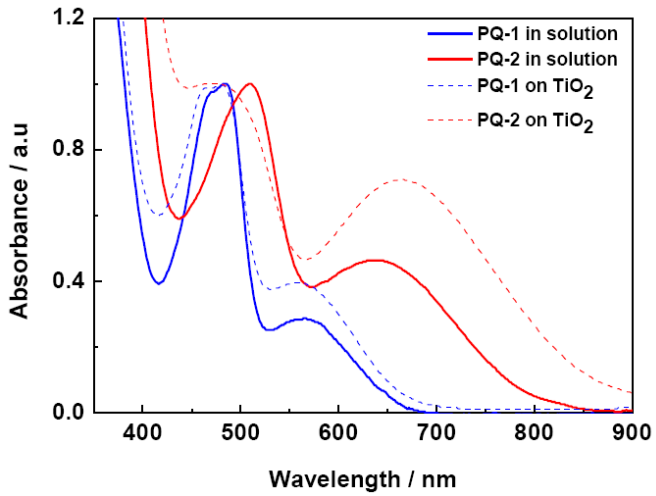

Figure 2. Normalized absorption spectra of **PQ-1** (blue) and **PQ-2** (red) in dilute CH_2Cl_2 solution (straight line) and on thin TiO_2 film (dashed line).

Results and discussion

Optical and electrochemical properties

As an example, the synthetic route to **PQ-1** is schematically presented in Scheme 1. The UV-vis absorption spectra of **PQ-1** and **PQ-2** in dichloromethane solution are presented in Figure 2. Both **PQ-1** and **PQ-2** exhibited the similar absorption features with two absorption bands in the visible region. The band at 484 nm (**PQ-1**) or 510 nm (**PQ-2**) corresponds to the π–π* transition of the conjugated system. The longest wavelength absorption of **PQ-1** (λ_{max} = 565 nm) is assigned to a charge transfer (CT) transition, being significantly blue-shifted compared to the CT-band of **PQ-2** (λ_{max} = 638 nm). The blue-shift means a larger torsion produced at the both ends of the pyrazino[2,3-g]quinoxaline with the two adjacent phenyl units in **PQ-1** than with the two thienyls in **PQ-2**. The absorption spectra of both the dyes adsorbed on 3 micrometer transparent TiO_2 films show feature similar to those in the corresponding solutions. **PQ-2**, however, shows a large red-shft of 26 nm mainly due to the strong aggregation on TiO_2 surface. Their fluorescence emission spectra were recorded as shown in Figure S1. The photophysical properties of the two dyes are summarized in Table 1.

Cyclic voltammetry measurements were performed in a 0.1 M dichloromethane solution of tetra-*n*-butylammonium hexafluorophosphate with ferrocene as internal standard at 0.63 V *vs.* NHE. As shown in Figure 3, the first oxidation potentials ($E_{+/0}$) of **PQ-1** and **PQ-2** were observed to be 0.93 and 0.95 V *vs*. NHE, respectively, which are assigned to the oxidation of the triphenylamine unit. Both the potential values are substantially more positive than the iodide/triiodide couple redox (0.4 V *vs.* NHE), indicating that the ground-state sensitizer regeneration is energetically favourable for DSCs.[9a] The optical transition energies ($E_{0\text{-}0}$) were 1.84 eV for **PQ-1** and 1.48 eV for **PQ-2**, estimated by using the onset of the UV-vis spectra in dichloromethane. The excited-state redox potential, $E_{+/*}$, determined by subtracting $E_{0\text{-}0}$ from $E_{+/0}$, were –0.91 V for **PQ-1** and –0.53 V for **PQ-2**. The value of –0.91 V for **PQ-1** is negative enough to allow their excited-state electron transfer into the TiO_2 conduction band (–0.5 V *vs.* NHE),[10a] while the high value of –0.53 V for **PQ-2** may imply a deficient driving force for the electron transfer.

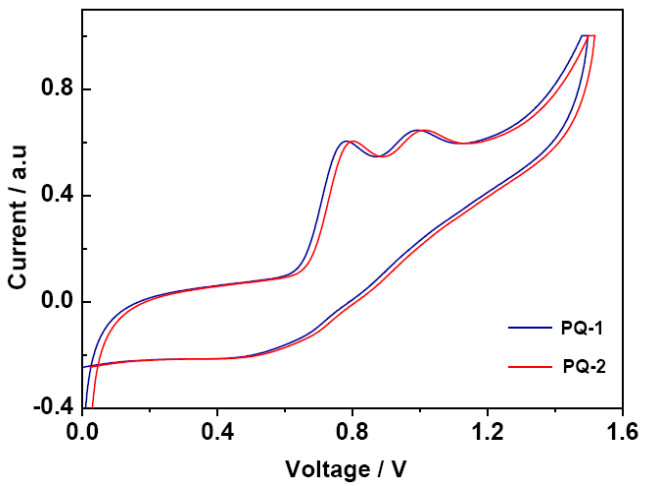

Figure 3. Oxidative cyclic voltammetry plots of **PQ-1** and **PQ-2** in in a 0.1 M dichloromethane solution of tetra-*n*-butylammonium hexafluorophosphate.

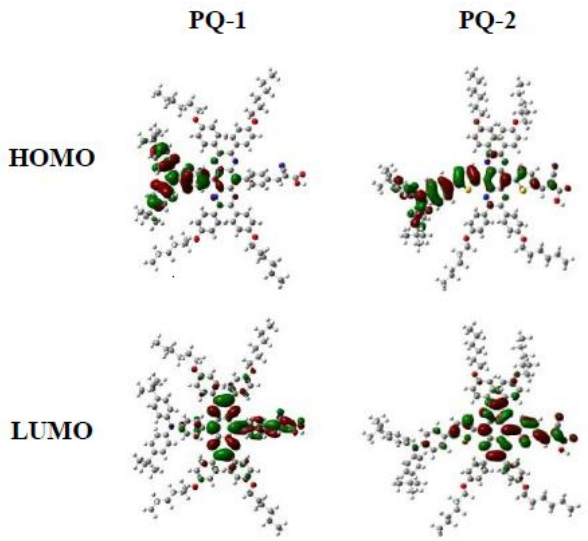

Figure 4. Schematic diagrams of the frontier molecular orbitals of **PQ-1** and **PQ-2** calculated at the B3LYP/6-31g (d,p) level of theory.

Density functional theory calculations

In order to get insight into the geometrical configuration and electron distribution of the frontier orbitals of the two dyes, density functional theory (DFT) calculations were made on a

B3LYP/6-31G level. Their optimized ground state molecular structures and corresponding dihedral angles were presented in the Supporting Information. In the structure of **PQ-1**, the dihedral angles of the pyrazino[2,3-g]quinoxaline with the two

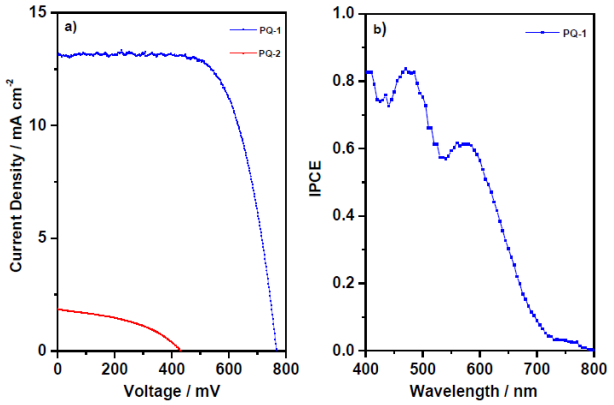

Figure 5. (a) *J-V* characteristic of DSCs sensitized by **PQ-1** and **PQ-2** measured under illumination with simulated AM 1.5G sunlight (b) IPCE spectrum of the DSC sensitized by **PQ-1.**

neighbouring phenyl rings are 46.8 ° and 49.9 °, while in the case of **PQ-2,** the dihedral angles of the pyrazino[2,3-g]quinoxaline with the two adjacent thienyl rings are 15.3 ° and 15.4 °. It is clear that **PQ-2** is much more planar in molecular configuration than **PQ-1**. Naturally more planar **PQ-2** favors a broad electron density distribution of the HOMO and LUMO orbitals as compared to **PQ-1,** as shown in Figure 4. In addition, the significantly red-shifted spectrum of **PQ-2** observed in Figure 2 could result from its high planar characteristic that would cause an efficient charge transfer from the donor to the acceptor. On the other hand, the dye molecules with planar configuration may deteriorate the device performances due to their potential aggregation on the TiO_2 surface.

Solar cell performance

Photovoltaic performance of **PQ-1** and **PQ-2** dyes as sensitizers for DSCs was tested with liquid electrolytes. Double-layer TiO_2 films were employed for dye adsorption. In the case of no CDCA co-adsorbant in dye solutions, the **PQ-1** based device gave a short circuit current density (J_{sc}) of 10.25 mA/cm^2, an open circuit voltage (V_{oc}) of 733 mV, and a fill factor (*FF*) of 0.64, corresponding to an overall conversion efficiency (η) of 4.81%, while the **PQ-2** based device gave J_{sc} of 1.12 mA/cm^2, V_{oc} of 422 mV, *FF* of 0.41, and η of 0.19%. With the addition of the CDCA in the dye solutions, the performance of the **PQ-1** based device improved significantly. At the optimized condition of 20 mM CDCA, the **PQ-1** based device gave a J_{sc} of 13.13 mA/cm^2, a V_{oc} of 768 mV, a *FF* of 0.68 with η of 6.86%, while the **PQ-2** based device gave J_{sc} of 1.86 mA/cm^2, V_{oc} of 432 mV, *FF* of 0.43, and η of 0.34%, as shown in Figure 5a. The dye amounts on TiO_2 films were comparable for **PQ-1** (1.50×10^{-7} mol cm^{-2}) and **PQ-2** (1.71×10^{-7} mol cm^{-2}) in the devices. The results indicate that PQ-1 and PQ-2 dyes with the lateral bulky alkoxy-substituted phenyl units are still inclined to aggregate on TiO_2 films, and the CDCA co-adsorbant can effectively reduce the tendency. Both the device efficiencies were found to decrease with further increasing CDCA content, mainly due to the decrease of the photcurrent. Under the same conditions without CDCA, the N719-based DSC gave J_{sc} of 18.22 mA/cm^2, V_{oc} of 728 mV, *FF* of 0.69 and η of 9.15%. Considering the low LUMO levels of PQ-2 (- 0.53V), we tried to increase the content of LiI (0.3M) in the electrolytes with no 4-*tert*-butylpyridine in order to shift the TiO_2 conduction band downward for efficient charge transfer, but there is no considerable improvement in the performance (J_{sc}, V_{oc}, *FF and* η are 2.24 mA/cm^2, 428 mV, 0.48, 0.46%, respectively). The poor efficiency for **PQ-2** comes from all the poor parameters (J_{sc}, V_{oc} and *FF*), and may be explained by the low driving force between its excited-state redox potential and the TiO_2 conduction band as mentioned above. In addition, the high planar configuration of **PQ-2** may cause the dye strong aggregation on the TiO_2 surface and thus deteriorate the device performances.[16] The results indicate that the energy level alignment is important in the design of low-band dye in the DSC system.[17-18] The further molecular modification of the indigo-based dyes is under progress.

Figure 5b provides an action spectrum (IPCE), which is consistent with the absorption spectra shown in Figure 2. The **PQ-1** based device clearly exhibited a stronger and broader response in the entire visible spectral region.

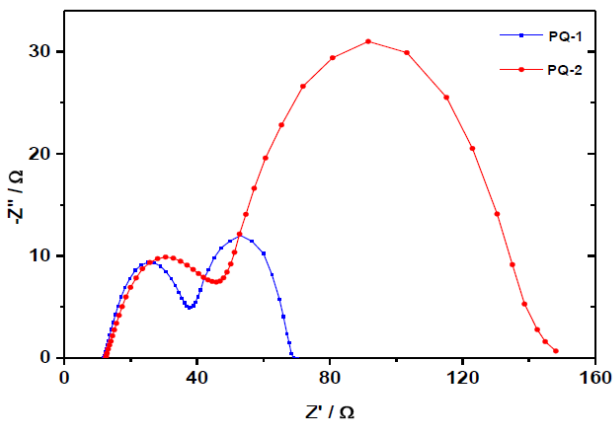

Figure 6. Electrochemical impedance spectra measured in the dark at a forward bias of 0.70 V for the DSCs employing **PQ-1** and **PQ-2**.

For further elucidating the large difference in performance for **PQ-1** and **PQ-2**, electrochemical impedance spectroscopy (EIS) was performed to investigate the FTO/TiO_2/dye interfaces. The Nyquist plots of DSCs were recorded in the dark with a forward bias of 0.70 V, as shown in Figure 6. Two semicircles from left to right in the Nyquist plot were assigned to the resistances of charge transfer (R_{Pt}) on the Pt counter electrode and charge recombination (R_r) at the interface of the TiO_2/electrolyte. It is clear that the semicircle for R_r is much larger in **PQ-2** than that in **PQ-1**, which may indicate inefficient charge transfer at the TiO_2/**PQ-2** dye interface due to

the low driving force for electron injection from the excited dye to TiO_2 as mentioned above.

Conclusions

In conclusion, two new pyrazino[2,3-g]quinoxaline-based dyes, **PQ-1** and **PQ-2**, have been designed, prepared and employed as sensitizers in DSCs. Our results demonstrated that the pyrazino[2,3-g]quinoxaline unit is a promising π-linker for the construction of low band gap sensitizers in DSCs. In the DSCs, **PQ-1** gave a power conversion efficiency of 6.86%, while more planar **PQ-2** gave only 0.34% at the same conditions. This work may provide a valuable, basic guideline for rational design of D–π–A molecules for high performance DSCs.

Acknowledgements

The authors greatly appreciate the financial support from National Natural Science Foundation of China (Project No. 21102150) for financial support of this work.

Notes and references

[a] *Beijing National Laboratory for Molecular Sciences(BNLMS), Key Laboratory of Green Printing, Institute of Chemistry, Chinese Academy of Sciences, Beijing, 100190, China*
[b] *Graduate School of Chinese Academy of Sciences, Beijing 100049, China*
Electronic Supplementary Information (ESI) available: Synthesis details and characterization. See DOI: 10.1039/b000000x/

1. B. O'regan, M. Grätzel, *Nature*, 1991, **353**, 737.
2. (a) M. K. Nazeeruddin, F. D. Angelis, S. Fantacci, A. Selloni, G. Viscardi, P. Liska, S. Ito, B. Takeru, M. Grätzel, *J. Am. Chem. Soc*,. 2005, **127**, 16835. (b) Y. Chiba, A. Islam, Y. Watanabe, R. Komiya, N. Koide, L. Han, *Jpn. J. Appl. Phys.*, 2006, **45**, L638. (c) F. F. Gao, Y. Wang, D. Shi, J. Zhang, M. K. Wang, X. Y. Jing, R. Humphry-Baker, P. Wang, S. M. Zakeeruddin, M. Grätzel, *J. Am. Chem. Soc*., 2008, **130**, 10720.
3. (a) K. Hara, K. Sayama, Y. Ohga, A. Shinpo, S. Suga, H. Arakawa, *Chem. Commun.*, 2001, 569. (b) S. Kim, J. K. Lee, S. O. Kang, J. Ko, J. H. Yum, A. Fantacci, F. D. Angelis, D. Di Censo, M. K. Nazeeruddin, M. Grätzel, *J. Am. Chem. Soc*., 2006, **128**, 16701. (c) Y. Bai, J. Zhang, D. F. Zhou, Y. H. Wang, M. Zhang, P. Wang, *J. Am. Chem. Soc*., 2011, **133**, 11442. (d) S. L. Li, K. J. Jiang, K. F. Shao, L. M.Yang, *Chem. Commun.*, 2006, 2792. (e) T. Horiuchi, H. Miura, K. Sumioka, S. Uchida, *J. Am. Chem. Soc*., 2004, **126**, 12218. (f) D. P. Hagberg, T. Edvinsson, T. Marinado, G. Boschloo, A. Hagfeldt, L. C. Sun, *Chem. Commun.*, 2006, 2245. (g) A. Yella, H.-W. Lee, H. N. Tsao, C. Y. Yi, A. K. Chandiran, M. K. Nazeeruddin, E. W. G. Diau, C.-Y. Yeh, S. M. Zakeeruddin, M. Grätzel, *Science*, 2011, **334**, 629; (h) K. Kurotobi, Y. Toude, K. Kawamoto, Y. Fujimori, S. Ito, P. Chabera, V. Sundström, H. Imahori, *Chem. Eur. J.*, 2013, **19**, 17075; (i) S. Mathew, A. Yella, P. Gao, R. Humphry-Baker, B. F. E. Curchod, N. Ashari-Astani, I. Tavernelli, U. Rothlisberger, Md. K. Nazeeruddin, M. Grätzel, *Nature Chem.*, 2014, **6**, 242.
4. (a) Y. Z. Wu, X. Zhang, W. Q. Li, Z.-S.Wang, H. Tian, W. H. Zhu, *Adv. Energy Mater*., 2012, **2**, 149; (b) S. Haid, M. Marszalek, A. Mishra, M. Wielopolski, J. Teuscher, J.-E. Moser, R. Humphry-Baker, S. M. Zakeeruddin, M. Grätzel, P. Bäuerle, *Adv. Funct. Mater*., 2012, **22**, 1291; (c) M. Velusamy, J. K. R. Thomas, J. T. Lin, Y.-C. Hsu, K.-C. Ho, *Org. Lett.*, 2005, **7**, 1899.
5. (a) Y. Cui, Y. Z. Wu, X. F. Lu, X. Zhang, G. Zhou, F. B. Miapeh, W. H. Zhu, Z.-S. Wang, *Chem. Mater.*, 2011, **23**, 4394; (b) Y.-S. Yen, C.-T. Lee, C.-Y. Hsu, H.-H. Chou, Y.-C. Chen, J. T. Lin, *Chem. Asian J.*, 2013, **8**, 809.
6. (a) K. Pei, Y. Z. Wu, W. J. Wu, Q. Zhang, B. Q. Chen, H. Tian, W. H. Zhu, *Chem. Eur. J.*, 2012, **18**, 8190; (b) X. F. Lu, Q. Y. Feng, T. Lan, G. Zhou, Z.-S. Wang, *Chem. Mater*., 2012, **24**, 3179; (c) D. W. Chang, H. J. Lee, J. H. Kim, S. Y. Park, S. M. Park, L. M. Dai, J. B. Baek, *Org. Lett.*, 2011, **13**, 3880; (d) X. F. Lu, X. W. Jia, Z.-S. Wang, G. Zhou, *J. Mater. Chem. A*, 2013, **1**, 9697;(e) J. B. Yang, P. Ganesan, J. Teuscher, T. Moehl, Y. J. Kim, C. Y. Yi, P. Comte, K. Pei, T. W. Holcombe, M. K. Nazeeruddin, J. L. Hua, S. M. Zakeeruddin, H. Tian, M.Grätzel, *J. Am. Soc. Soc.*, 2014, **136**, 5722.
7. (a) T. W. Holcombe, J.-H. Yum, J. Yoon, P. Gao, M. Marszalek, D. D. Censo, K. Rakstys, M. K. Nazeeruddin, M. Gätzel, *Chem. Commun.*, 2012, **48**, 10724; (b) S. Y. Qu, W. J. Wu, J. L. Hua, C. Kong, Y. T. Long, H. Tian, *J. Phys. Chem. C.*, 2010, **114**, 1343.
8. (a) Y. R. Shi, R. B. M. Hill, J.-H. Yum, A. Dualeh, S. Barlow, M. Gätzel, S. R. Marder, M. K. Nazeeruddin, *Angew. Chem. Int. Ed.*, 2011, **50**, 6619;(b) J.-H. Yum, P. Walter, S. Huber, D. Rentsch, T. Geiger, F. Nüesch, F. D. Angelis, M. Grätzel, M. K. Nazeeruddin, *J. Am. Chem. Soc.*, 2007, **129**, 10320.
9. (a) X. Lu, G. Zhou, H. Wang, Q. Feng, Z. S. Wang, *Phys Chem Chem Phys.*, 2012, **14**, 16779; (b) S. Erten-Ela, M. D. Yilmaz, B. Icli, Y. Dede, S. Icli, E. U. Akkaya, *Org. Lett*., 2008, **10**, 3299; (c) M. Gupta, S. Mula, M. Tyagi, T. K. Ghanty, S. Murudkar, A. K. Ray, S. Chattopadhyay, *Chem. Eur. J*., 2013, **19**, 17766.
10. (a) W. J. Ying, F. L. Guo, J. Li, Q. Zhang, W. J. Wu, H. Tian, J. L. Hua, *ACS Appl. Mater. Interfaces*, 2012, **4**, 4215; (b) S.-G. Li, K.-J. Jiang, J.-H. Huang, L.-M. Yang, Y.-L. Song, *Chem. Commun.*, 2014, **50**, 4309.
11. W. Q. Li, Y. Z. Wu, Q. Zhang, H. Tian, W. H. Zhu, *ACS Appl. Mater. Interfaces*, 2012, **4**, 1822.
12. (a) Q. Peng, X. J. Liu, Y. C. Qin, J. Xu, M. J. Li, L. M. Dai, *J. Mater. Chem.*, 2011, **21**, 7714; (b) M. Mastalerz, V. Fischer, C.-Q. Ma, René A. J. Janssen, P. Bäuerle, *Org. Lett*, 2009, **11**, 4500.
13. D. G. (Dan)Patel, F. D. Feng, Y.-Y Ohnishi, K. A. Abboud, S. Hirata, K. S. Schanze, J. R. Reynolds, *J. Am. Chem. Soc.* 2012, **134**, 2599.
14. P. Wang, S. M. Zakeeruddin, P. Comte, R. Charvet, R. Humphry-Baker, M. Grätzel, *J. Phys. Chem. B*, 2003, **107**, 1436.
15. S. Ito, T. N.Murakami, P. Comte, P. Liska, C. Grätzel, M. K. Nazeeruddin, M. Grätzel, *Thin Solid Films*, 2008, **516**, 4613.
16. (a) B. Lim, G. Y. Margulis, J.-H. Yum, E. L. Unger, B. E. Hardin, M. Grätzel, M. D. MeGehee, A. Sellinger, *Org. Lett.*, 2013, **15**, 784; (b) I. López-Duarte, M. Wang, R. Humphry-Baker, M. Ince, M. V. Martínez-Díaz, M. K. Nazeeruddin, T. Torres, M. Grätzel, *Angew. Chem., Int. Ed.*, 2012, **51**, 1895; (c) L. Yu, X. Zhou, Y. Yin, Y. Liu, R. Li, T. Peng, *ChemPlusChem*, 2012, **77**, 1022.
17. S. Y. Qu, C. J. Qin, A. Islam, Y. Z. Wu, W. H. Zhu, J. L. Hua, H. Tian, L. Y. Han, *Chem. Commun.* 2012, **48**, 6972.
18. Y. Z. Wu, W. H. Zhu, *Chem. Soc. Rev.*, 2013, **42**, 2039

